frontiers | Frontiers in Marine Science

TYPE Original Research
PUBLISHED 19 August 2022
DOI 10.3389/fmars.2022.943100

OPEN ACCESS

EDITED BY
Daniel J. Mayor,
National Oceanography Centre,
United Kingdom

REVIEWED BY
Kathryn Barbara Cook,
University of Southampton,
United Kingdom
Marianne Wootton,
Marine Biological Association,
United Kingdom

*CORRESPONDENCE
Yunosuke Koguchi
makaroni1009@eis.hokudai.ac.jp

SPECIALTY SECTION
This article was submitted to Marine Ecosystem Ecology, a section of the journal Frontiers in Marine Science

RECEIVED 13 May 2022
ACCEPTED 28 July 2022
PUBLISHED 19 August 2022

CITATION
Koguchi Y, Tokuhiro K, Ashjian CJ, Campbell RG and Yamaguchi A (2022) Inter-species comparison of the copepodite stage morphology, vertical distribution, and seasonal population structure of five sympatric mesopelagic aetideid copepods in the western Arctic Ocean.
Front. Mar. Sci. 9:943100.
doi: 10.3389/fmars.2022.943100

Inter-species comparison of the copepodite stage morphology, vertical distribution, and seasonal population structure of five sympatric mesopelagic aetideid copepods in the western Arctic Ocean

Yunosuke Koguchi[1]*, Koki Tokuhiro[1], Carin J. Ashjian[2], Robert G. Campbell[3] and Atsushi Yamaguchi[1,4]

[1]Faculty/Graduate School of Fisheries Sciences, Hokkaido University, Hakodate, Japan, [2]Biology Department, Woods Hole Oceanographic Institution, Woods Hole, MA, United States, [3]Graduate School of Oceanography, University of Rhode Island, Narragansett, RI, United States, [4]Arctic Research Center, Hokkaido University, Sapporo, Japan

Aetideidae is a calanoid copepod family dominant in the mesopelagic layer of the Arctic Ocean for which little ecological information is available because species identification, especially of early copepodite stages, is difficult. In this study, we developed a species identification flow for the whole copepodite stages of five sympatric aetideid copepods (*Chiridius obtusifrons*, *Gaetanus tenuispinus*, *G. brevispinus*, *Aetideopsis multiserrata*, and *A. rostrata*). Vertical distributions and seasonal population structures of these species were evaluated using a year-round sample time-series collected at the drifting ice station (SHEBA) in the western Arctic Ocean. Combinations of morphological characteristics (prosome length, cephalosome, and prosome widths) were used to identify the early copepodite stages to species. *Aetideopsis rostrata* was distributed in deep waters (1,032–1,065 m) throughout the year. The other species all were found at 600–700 m during the midnight sun. However, during the polar night, the vertical distributions of each species were distinct, resulting from ascent, descent, or depth maintenance, indicating seasonal vertical migration which may function to reduce inter-specific competition during the polar night when food resources are scarce. Reproduction timing varied among four aetideid copepods: *C.obtusifrons* and *G. tenuispinus* showed polar night ascent and reproduction at the end of the polar night, whereas *G. brevispinus* and *A. multiserrata* showed descent or depth maintenance during the polar night and reproduction at the beginning of the polar night. There was not sufficient data to examine reproduction timing of *A. rostrata*. Common for all aetideid species, $\delta^{15}N$ values of the adult females indicate more carnivorous feeding modes during the polar night than those in

the midnight sun. Such vertical distribution and timing of reproduction variation among these five aetideid copepods may function to reduce species competition in the mesopelagic layer of the Arctic Ocean.

KEYWORDS

Aetideidae, sympatric mesopelagic copepods, vertical distribution, population structure, reproduction, the Arctic Ocean

1 Introduction

In the Arctic Ocean marine ecosystem, the zooplankton community is an important secondary producer and plays a role in energy transfer to higher trophic level organisms as well as mediating vertical material transportation (Lowry et al., 2004; Wassmann et al., 2006). Copepods are the dominant taxon of the zooplankton community in the Arctic Ocean (Thibault et al., 1999; Ashjian et al., 2003). Because of seasonal ice coverage, most information about Arctic Ocean copepod ecology has been obtained during the summer (under midnight sun conditions) (cf. Laakmann et al., 2009a), and few studies have been conducted to investigate copepod ecology during the winter (under polar night conditions) (Zhang et al., 2010). Consequently, ecological and standing stock information about the Arctic copepods during the winter and their seasonal changes is scarce. To fill this knowledge gap, we considered that zooplankton sampling conducted from the drifting ice station in the Arctic could facilitate the year-round observation of standing stocks, population structure, and vertical distribution of Arctic copepods (Ashjian et al., 2003).

Most of the existing ecological information on Arctic planktonic copepods is available for surface-dwelling, numerically dominant copepod species (e.g., *Pseudocalanus* spp.) and interzonal, particle-feeding copepods that have a diapause phase at deeper depths (e.g., *Calanus* spp.). However, the species diversity of copepods is known to be high in the deep sea, especially in the mesopelagic zone (Lee, 2000; Norris, 2000; Goetze, 2003). The Aetideidae is a family of copepods that dominates the copepod community in the mesopelagic zone, and is characterized by a high species diversity (Richter, 1995; Markhaseva, 1996; Auel, 1999). Members of the Aetideidae are known to be omnivores or detritivores and are described as opportunistic feeders (Richter, 1995; Auel, 1999; Sano et al., 2013; Sano et al., 2015). The occurrence of species-specific food preferences (Laakmann et al., 2009a; Laakmann et al., 2009b; Sano et al., 2013; Sano et al., 2015) and species-specific vertical segregation within the family (Kosobokova and Hirche, 2000; Auel and Hagen, 2002; Laakmann et al., 2009a; Smoot and Hopcroft, 2017) is well documented. Although the hydrographic condition of the deep Arctic Ocean is homogenous (cold and fresh), coexistence of Aetideidae species is thought to occur by vertical and food segregation (Laakmann et al., 2009a; Laakmann et al., 2009b; Laakmann and Auel, 2010). Stable isotopes especially $\delta^{15}N$ are a useful guide for food preference (Laakmann et al., 2009a; Laakmann et al., 2009b; Laakmann and Auel, 2010). Mesopelagic copepods are reported to have a substantial effect on vertical material flux to the deep sea by feeding on sinking particles and excretion in the form of faecal pellets (Dilling et al., 1998; Wilson et al., 2010), and aetideid copepods in the Greenland Sea are reported to consume 40% of the particulate organic carbon flux that reaches at their habitat depth (Auel, 1999). These facts suggest that Aetideidae is an important copepod taxon in the Arctic Ocean, both from species diversity and vertical material flux perspectives.

A key challenge to conducting an ecological study of Aetideidae is the difficulty of species identification, especially for the early copepodite stages (C1–C3). In part, this is because morphological identification keys for each sympatric species have not yet been created, and the early copepodite stages of the Aetideidae have been treated as *aetideid copepods C1–C3* in previous studies conducted in the Arctic Ocean (e.g., Kosobokova and Hirche, 2000; Auel and Hagen, 2002). Consequently, little is known about the life history, seasonal population structure, and timing of reproduction of the aetideid copepods in the Arctic Ocean. To improve our knowledge of the ecology of aetideid copepods, it is necessary to create species identification criteria based on morphological characteristics of all the copepodite stages.

In this study, we examined a year-round time series of zooplankton samples collected from the drifting *Surface Heat Budget of the Arctic Ocean* (SHEBA) ice station in the western Arctic Ocean. We conducted morphological identification of all the copepodite stages of five dominant sympatric aetideid copepods. We also determined the seasonal changes in the vertical distribution and population structure of these five species. We measured $\delta^{15}N$ of adult females of all aetideid copepods with midnight sun and polar night for evaluation of their food preference. We compared the seasonal dynamics of the five sympatric aetideid copepods and considered the

mechanism of coexistence of these copepod species in the mesopelagic layer of the Arctic Ocean.

2 Materials and methods

2.1. Field sampling

Zooplankton sampling was conducted from the drifting SHEBA ice station from 27 October 1997 to 29 September 1998. Vertical stratification samples were collected from 2–7 depth layers over a depth range of 0–3,500 m depth using a closing net with a 1 m^2 mouth area and 150 μm or 53 μm mesh. The small mesh (53 μm) was used for the shallow samples (<200 m) of the restricted period (February-August 1998). Samples were collected at 10–14 day intervals (Figure 1). The SHEBA ice station drifted from the Canadian Basin to the Mendeleyev Basin during the one-year sampling period (Ashjian et al., 2003). Because of this drift, the water depth varied from 352 m to 3,800 m during the sampling period, consequently, the zooplankton collection depth and the number of layers sampled ranged from 0–100 m to 0–3,500 m and from 2 to 7 layers, respectively. The details of the sampling layer at each sampling date are available in Ashjian and Campbell (2007). The zooplankton samples were preserved using 4% buffered formaldehyde seawater. On each sampling day, water temperature, salinity, and chlorophyll *a* (Chl. *a*) fluorescence values were measured for the upper water column (maximum depth: 300 or 700 m) with a SeaBird SB11 Seacat CTD (SeaBird Scientific, Bellevue, WA, USA), equipped with a calibrated fluorometer. Daylight hours for each sampling day were calculated based on the latitude of the sampling site (cf. Brock, 1981).

2.2. Microscope observations

Using a stereomicroscope, each copepodite stage of the five dominant aetideid copepods (*Chiridius obtusifrons*, *Gaetanus tenuispinus*, *G. brevispinus*, *Aetideopsis multiserrata*, and *A.*

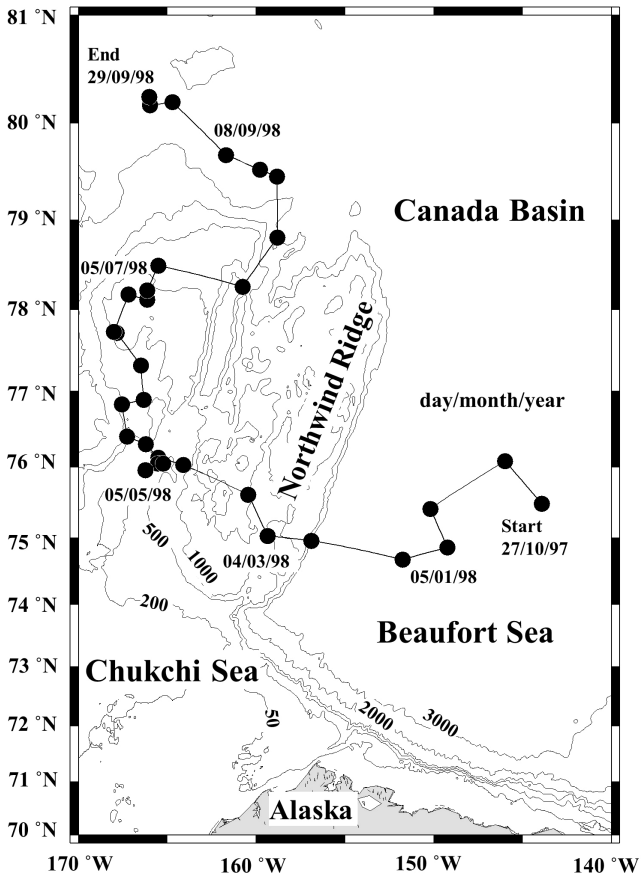

FIGURE 1
Location of the zooplankton sampling sites (black circles) along the drift track of the Surface Heat Budget of the Arctic Ocean (SHEBA) ice station through the Canada Basin to the Mendeleev Plain from 27 October 1997 to 29 September 1998 (cf. Ashjian et al., 2003).

rostrata) was identified and enumerated. Based on the presence (male) or absence (female) of a fifth swimming leg, males and females were distinguishable for specimens of the C4–C6 stages (hereafter referred to as C4F–C6F and C4M–C6M). We provide a flow diagram showing species identification of the whole copepodite stages of the aetideid copepods in Table 1.

For species identification of stages C4–C6, we used the shape of the spine at the end of the thoracic segment (Brodskii, 1950). Since the shape of the spine was similar for *C. obtusifrons* and *Aetideopsis* spp., we used the number of thoracic segments (three for *C. obtusifrons* and four for *Aetideopsis*) which was identifiable from the dorsal view as an identification guide (Figure 2). For the congener species, body sizes determined as prosome length (PL) varied: for *Gaetanus* spp., *G. brevispinus* was larger than *G. tenuispinus*, and for *Aetideopsis* spp., *A. rostrata* was larger than *A. multiserrata*. Because the spine at the end of the thoracic segment was not developed in stages C1–C3, we used the cephalosome width around the antenna (CW_{A2}) and cephalosome width around the mandible (CW_{Md}) (Figure 2) as alternative species-identification characteristics for C1–C3. The cephalosome outer margin of *Gaetanus* was smooth, whereas the outer margins of *Chiridius* and *Aetideopsis* were expanded around the antenna. Based on these morphological features, the C1–C3 copepodite stages were identified to the genus level based on the CW_{A2}: CW_{Md} ratio, thus, a specimen with a large CW_{A2}: CW_{Md} ratio was identified as *Chiridius* and *Aetideopsis*, and specimens with a small CW_{A2}: CW_{Md} ratio as *Gaetanus*. Identification of species within a genus was based on PL. Because the C1–C3 stages of *C. obtusifrons* and *A. multiserrata* were similar in PL and morphology of the outer cephalosome margin, we observed the prosome width at the middle of the prosome (PW) and identified large PW specimens as *C. obtusifrons* and small PW specimens as *A. multiserrata*. To define the size ranges used to discriminate species (Figure 4), the PL, CW_{A2}, and CW_{Md} were measured for 5–10 individuals of each copepodite stage of each species sorted from the most abundant samples under a stereomicroscope using an eyepiece micrometre with a precision of 10 μm. For the C1–C3 stages of *C. obtusifrons* and *A. multiserrata*, PW was also measured. For means, standard deviations, and ranges of each parameter (PL, PW, CW_{A2}, CW_{Md}, and CW_{A2}: CW_{Md}) at each stage, we provide the data in Supplementary Tables 1–9.

It should be noted that the identification for the juvenile copepodite stages of this study is not confirmed by molecular identification. Thus, the identification should be termed the open nomenclature term incerta (Horton et al., 2021) to indicate uncertain identification (e.g. *C. obtusifrons* sp. inc., *G. tenuispinus* sp. inc., *G. brevispinus* sp. inc., *A. multiserrata* sp. inc., and *A. rostrata* sp. inc.).

TABLE 1 Flow diagram for species identification on juvenile copepodite stages of five sympatric Aetideidae copepods (*Chiridius obtusifrons, Gaetanus tenuispinus, Gaetanus brevispinus, Aetideopsis multiserrata*, and *Aetoideopsis rostrata*) in the western Arctic Ocean.

Stages	Observation point	Figure references
C4–C5	•The shape of the spine at end of the thoracic segment (Brodskii, 1950)	2
	•Number of the thoracic segments in dorsal view	2
	Three → *C. obutusifrons*	
	Four → *Aetideopsis* spp.	
	•Within the genera, PL was varied with species.	4A
	Gaetanus spp.	
	Large PL → *G. brevispinus*	
	Small PL → *G. tenuispinus*	
	Aetideopsis spp.	
	Large PL → *A. rostrata*	
	Small PL → *A. multiserrata*	
C1–C3	•Cephalosome outer margin in dorsal view (CW_{A2}: CW_{Md})	4A
	Expanded around the antenna (large CW_{A2}: CW_{Md})	
	→ *C. obutusifrons* and *Aetideopsis* spp.	
	Smooth (small CW_{A2}: CW_{Md})	
	→ *Gaetanus* spp.	
	•Within *Gaetanus*, PL was varied with species.	4A
	Large PL → *G. brevispinus*	
	Small PL → *G. tenuispinus*	
	•PW was varied with species.	4B
	Large PW → *C. obtusifrons*	
	Small PW → *A. multiserrata*	

Prosome length: PL, cephalosome width around the antenna: CW_{A2}, cephalosome width around the mandible: CW_{Md}, prosome width: PW. For means, standard deviations, and ranges of each parameter (PL, PW, CW_{A2}, CW_{Md}, and CW_{A2}:CW_{Md}) in each stage, we provided the data in Supplementary Tables 1–9.

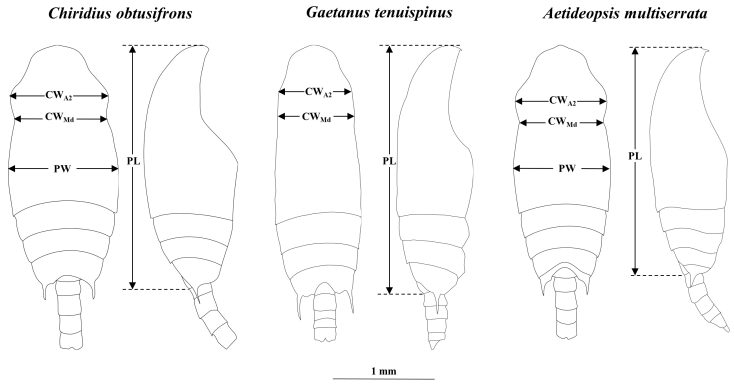

FIGURE 2
Diagrams showing body size measurements: cephalosome width at antenna (CW$_{A2}$), cephalosome width at mandible (CW$_{Md}$), prosome width at middle of the prosome (PW), and prosome length (PL) for *Chiridius obtusifrons* (left), *Gaetanus tenuispinus* (centre) and *Aetideopsis multiserrata* (right). Scale bar represents 1 mm.

2.3. Population structure

The depth topography below the ice station varied temporally as a consequence of drift, and this determined the maximum sampling depth on any one sampling day. Because Aetideidae species are distributed in the mesopelagic layer (Kosobokova and Hopcroft, 2010; Kosobokova et al., 2011), shallower sampling depths on some sampling days may have resulted in failure to collect representative samples of the Aetideidae populations at every sampling site. The likelihood of this is evidenced by the low abundance of Aetideidae species at the shallower sampling depths (see Supplementary Tables 10–13). Therefore, we used population structure data of the four species: *C. obtusifrons*, *G. tenuispinus*, *G. brevispinus*, and *A. multiserrata* only from sampling sites where the maximum sampling depths were greater than 500 m and omitted the data for the shallower sampling depths (<500 m maximum sampling depth) (Supplementary Tables 10–13). This resulted in a reduction in the number of sampling days from 30 to 19; however, the reduced data set comprised approximately one-month intervals, except for July 1998. The impact of maximum sampling depth was most severe for the deepest dwelling species, *A. rostrata*, and population structure data collected at depths shallower than 900 m were omitted for this species (Supplementary Table 14). As a result, time-series data for *A. rostrata* were not available from April to July 1998. To reduce the abrupt changes in the population structure data related to hydrographic and geographical changes, we standardized the abundance data for each copepodite stage by calculating the moving average of three consecutive sampling dates. For each sampling date, the mean copepodite stage (MCS) was calculated using the following formula (Marin, 1987):

$$MCS = \frac{\sum_{i=1}^{6} i \times A_i}{\sum_{i=1}^{6} A_i}$$

where i is the number of copepodite stages (1 for C1, 6 for C6) and Ai is the number of individuals at copepodite stage i (ind. m^{-2}).

2.4. Vertical distribution

The vertical distribution core ($D_{50\%}$) where 50% of the population was distributed, was calculated based on abundances (ind. m^{-2}) in each sampling layer (Pennak, 1943):

$$D_{50\%} = d_1 + (d_2 - d_1) \times \frac{50 - p_1}{p_2}$$

where d_1 is the depth (m) of the upper depth of the 50% individual occurrence layer, d_2 is the maximum depth (m) of the 50% individual occurrence layer, p_1 is the cumulative individual percentage (%) that occurred at depths shallower than the 50% individual occurrence layer, and p_2 is the individual percentage (%) at the 50% individual occurrence layer. The difference in $D_{50\%}$ between the polar night and midnight sun for all copepodite stages of each species was tested using the Mann-Whitney U-test. Differences in $D_{50\%}$ among copepodite stages within a species during the same period (i.e., during the polar night and during the midnight sun) were tested by one-way ANOVA. In addition, differences in $D_{50\%}$ among species during the same period were tested by one-way ANOVA and a *post hoc* test (Tukey-Kramer test). For the evaluation of $D_{50\%}$, we excluded the sampling dates when the maximum depth of collection was shallower than 900 m for all species because Aetideidae species are distributed in the

mesopelagic layer. Excluding data based on this criterion, we analysed six sampling dates for the polar night and three sampling dates for the midnight sun for comparison of the vertical distribution of Aetideidae (Supplementary Tables 10–14).

2.5. $\delta^{15}N$ value

For evaluation of food preference, $\delta^{15}N$ value was measured for C6F of each species with polar night and midnight sun. From the most abundant samples at each period, the batches of C6F specimens (since 5 mg DW was required for each measurement, 9–18 individuals which varied with species were set for each batch) were sorted, rinsed with distilled water then dried in a 60°C oven for five hours. Dried samples were ground into a fine powder with a ceramic mortar and pestle and used for measurement of ^{15}N and ^{14}N by using an elemental analyzer/isotope-ratio mass spectrometer (Flash EA1112-Delta V Plus He-Flow System, Thermo Fisher Scientific, Germany). The measurements were made in triplicate (three batches). $\delta^{15}N$ was calculated from the following equation:

$$\delta^{15}N = (\left[(15N_{sample}/14N_{sample})/(15N_{standard}/14N_{standard})\right] - 1) \times 1000$$

where $^{15}N_{sample}$ and $^{14}N_{sample}$ are the values of the samples, and $^{15}N_{standard}$ and $^{14}N_{standard}$ are the values of the standard. Species differences in $\delta^{15}N$ values were tested by one-way ANOVA and Tukey-Kramer test. Temporal changes (polar night vs midnight sun) within the species were tested by Mann-Whitney *U*-test.

3 Results

3.1 Hydrography

Seasonal variations in the daily daylight length, water temperature, salinity, and Chl *a* fluorescence determined at the SHEBA ice station are shown in Figure 3. Based on the daylight length at the SHEBA ice station, the polar night was demarcated to have occurred from early November 1997 to early February 1998, and the midnight sun from late April to late August 1998. The remaining periods were defined as transition periods. The water temperatures ranged between −1.76 and 0.91°C, and were lower in the shallower water and higher at depth. The salinity range was 26.60–34.91, being lower near the surface, and the halocline was observed at a depth range of approximately 100–200 m throughout the year. The Chl. *a* fluorescence ranged from 0.002 to 4.259 and was high above a depth of 30 m from June to August. During the course of the drifting ice station, three water masses were present for the shallower depths (< 100 m), but the remaining deep waters contained Arctic Intermediate Water and Polar Intermediate Water throughout the year (Ashjian et al., 2003).

3.2. Morphological characteristics

Scatter plots showing the relationship between the CW_{A2}: CW_{Md} ratio and PL for each copepodite stage of the five aetideid copepods are shown in Figure 4A. For all copepodite stages except C6M, CW_{A2}: CW_{Md} was low (approximately 0.9–1) for *Gaetanus* spp., whereas this ratio was high (approximately 1–1.1) for *Chiridius* and *Aetideopsis* species. This finding reflected the morphological difference of the cephalosome outer margin which was fused around the antenna in *Chiridius* and *Aetideopsis* species, but smooth in *Gaetanus* spp. Note that some variability was present for CW_{A2}: CW_{Md} ratio, especially for early copepodite stages (C1 and C3). Within the congener species, PL varied with species, where, for *Gaetanus* spp., the PL of *G. brevispinus* was larger than that of *G. tenuispinus*, and for the *Aetideopsis* spp. the PL of *A. rostrata* was larger than that of *A. multiserrata*. It should be noted that CW_{A2}: CW_{Md} was similar for *C. obtusifrons* and *A. multiserrata*, while some overlap was present, the PL of *C. obtusifrons* was larger than that of *A. multiserrata*. For identification of *C. obtusifrons* and *A. multiserrata*, the number of thoracic segments was used for stages older than C4. For identification of earlier stages (C1–C3) of these species, PW was used, where a large PW distinguished *C. obtusifrons*, and a small PW distinguished *A. multiserrata* (Figure 4B). For means, standard deviations, and ranges of each parameter (PL, PW, CW_{A2}, CW_{Md}, and CW_{A2}: CW_{Md}) in each stage, we provide the data in Supplementary Tables 1–9.

3.3. Vertical distribution

The vertical distribution core ($D_{50\%}$) of each copepodite stage of the five studied Aetideidae species during the polar night and the midnight sun is shown in Figure 5. Within the same stages, significant differences in vertical distribution between the polar night and midnight sun were observed only for *C. obtusifrons* C6F ($p<0.05$, Mann-Whitney *U*-test). Within the same season, significant differences in vertical distribution between the copepodite stages of the same species were observed only for *A. rostrata* during the polar night ($p<0.05$, one-way ANOVA). Comparisons between species and temporal changes within species based on the mean $D_{50\%}$ of all the copepodite stages during the polar night and midnight sun are shown in Table 2. During the polar night, *C. obtusifrons* and *G. tenuispinus* distributed at the shallowest depths (298–381 m), whereas *G. brevispinus* and *A. multiserrata* occurred 300–400 m deeper (628–791 m), and *A. rostrata* showed the deepest distribution (1,065 m). In contrast, during the midnight sun,

10.3389/fmars.2022.943100

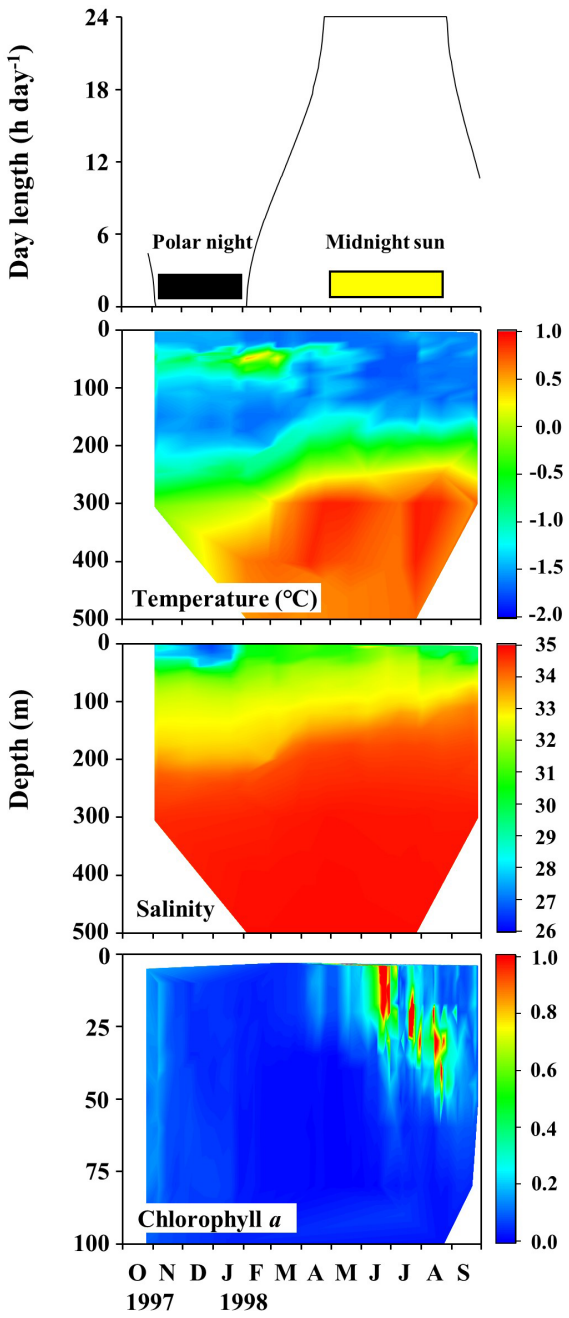

FIGURE 3
Seasonal changes in daylength, temperature, salinity, and chlorophyll *a* fluorescence recorded at the Surface Heat Budget of the Arctic Ocean (SHEBA) ice station as it drifted through the Canada Basin to the Mendeleev Plain from 27 October 1997 to 29 September 1998.

four of the species: *C. obtusifrons*, the two *Gaetanus* spp., and *A. multiserrata* distributed at similar depths (within a 100 m range), and only *A. rostrata* showed a significantly different distribution ($p<0.01$), at a depth approximately 300 m deeper than that of the other species. *C. obtusifrons* and *G. tenuispinus* showed shallower distributions during the polar night than during the midnight sun ($p<0.001$, Mann-Whitney *U*-test), whereas *G. brevispinus* showed a deeper distribution during the polar night compared to that during the midnight sun ($p<0.01$). The deepest dwelling species, the two *Aetideopsis* spp., showed no differences in their $D_{50\%}$ between the polar night and the midnight sun ($p>0.05$).

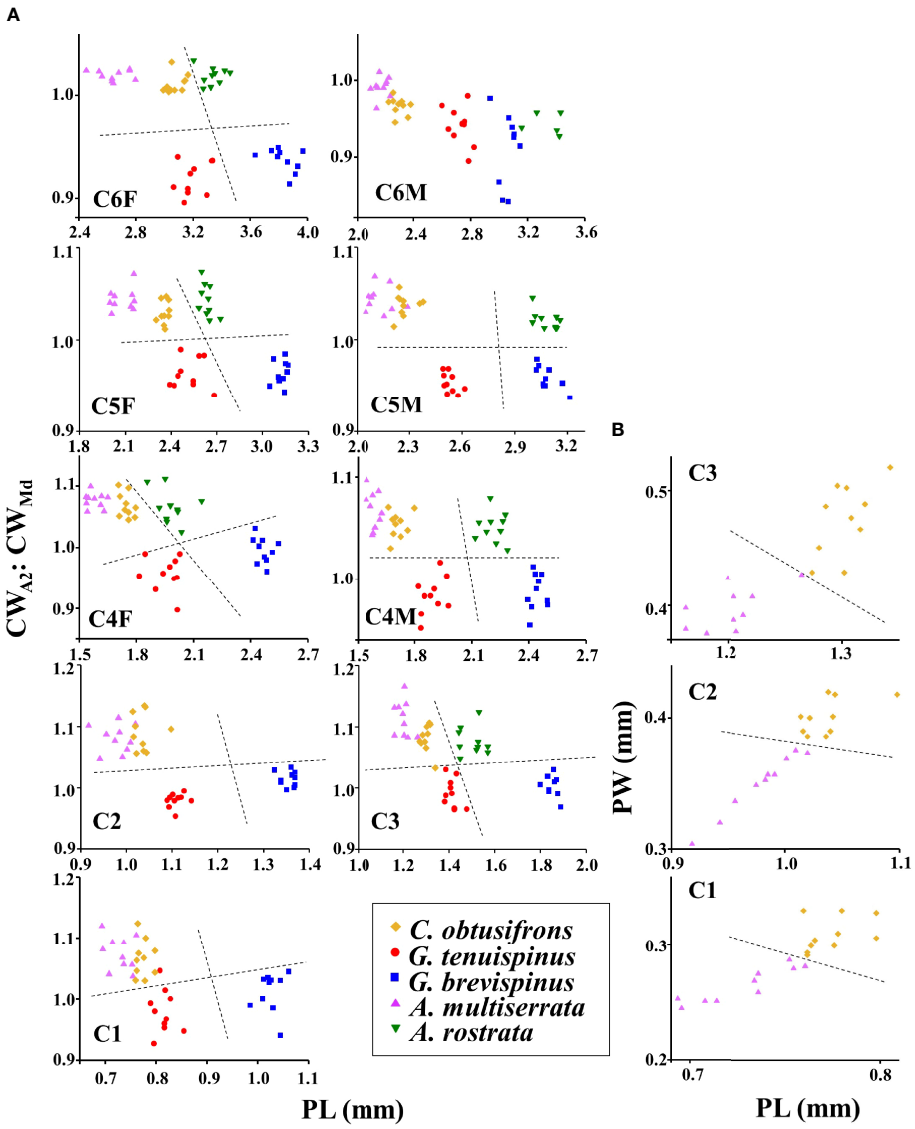

FIGURE 4
(A) Scatter plots of the ratio of the cephalosome width at the antenna (CW_{A2}): cephalosome width at the mandible (CW_{Md}) and the prosome length (PL) for each copepodite stage of the five Aetideidae copepods dominant in the western Arctic Ocean. The species are: *Chiridius obtusifrons*, *Gaetanus tenuispinus*, *G. brevispinus*, *Aetideopsis multiserrata*, and *A. rostrata*. **(B)** Scatter plots of prosome width (PW) and prosome length (PL) for the early copepodite stages of *C. obtusifrons* and *A. multiserrata*. F, female; M, male. Dashed lines represent approximate separation for each species at each copepodite stage. Because the scatter plots for *C. obtusifrons* and *A. multiserrata* in **(A)** were similar, additional plots were created for these two species in **(B)**.

3.4. Population structure

Seasonal changes in abundance, copepodite stage composition, MCS, and the proportion of C4–C6 in the female and male populations of the five aetideid copepods studied are shown in Figure 6. The season of peak abundance varied with species. The abundance of *C. obtusifrons* and *G. tenuispinus* was highest in May, whereas the abundance of *G. brevispinus* and *A. multiserrata* peaked in March. In all species, the MCS values were lowest when the recruitment of the early copepodite stages occurred. The lowest MCS value was observed in April–May for *C. obtusifrons* and *G. tenuispinus*, whereas it was recorded for *G. brevispinus* from January to March, and from February to March for *A. multiserrata*. The seasonal timing of early stage copepodite recruitment corresponded with the peak abundance seasons of each species. A common feature of all five species was a much lower proportion of C6 individuals in the male population compared to that in the female population. The proportion of

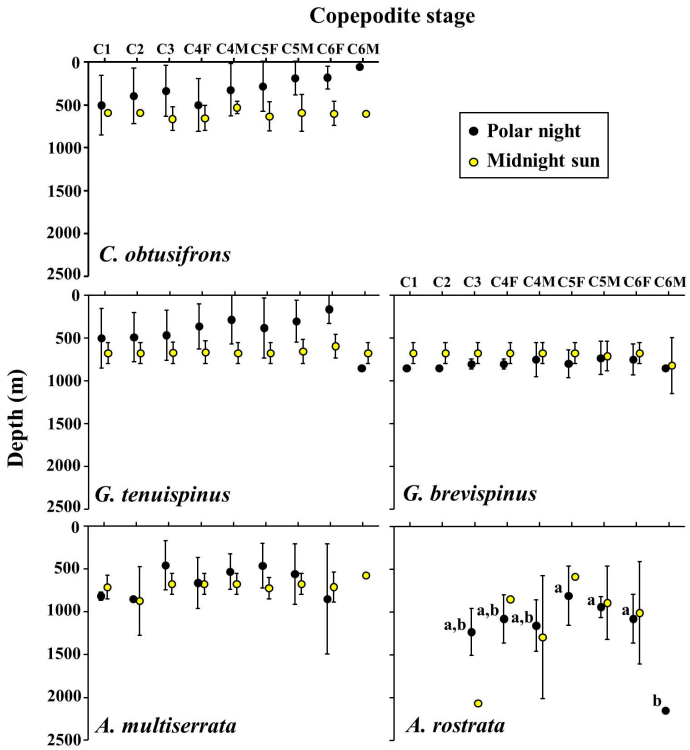

FIGURE 5
Ontogenetic changes in vertical distribution of the copepodite stages of the five Aetideidae copepods dominant in the western Arctic Ocean during the polar night and midnight sun. Symbols and bars represent means of the distribution centres ($D_{50\%}$) and their standard deviations, respectively. F, female; M, male. The species are: *Chiridius obtusifrons*, *Gaetanus tenuispinus*, *G. brevispinus*, *Aetideopsis multiserrata*, and *A. rostrata*. Alphabet letters for *A. rostrata* during the polar night indicate significant differences between stages.

females (%) in each copepodite stage (C4–C6) is shown in Table 3. For all species, females were dominant (56.6%–66.7%) in the C4–C6 populations, whereas males dominated the C4 and C5 populations. In all species, the C6 population was predominantly female (76.3%–97.3%), which may account for the higher overall proportion of females in the C4–C6 populations.

3.5. δ^{15}N value

δ^{15}N values of adult females of the aetideid copepods during the polar night and midnight sun are summarized in Table 4. During the polar night, δ^{15}N values were 14.1–16.4, with the lower values for *Gaetanus* spp. and higher values for *C. obtusifrons* and *Aetideopsis* spp. During the midnight sun,

TABLE 2 Summary of vertical distribution (vertical distribution core: $D_{50\%}$, mean ± SE) of five Aetideidae copepods in the western Arctic Ocean during the polar night and midnight sun.

Species	$D_{50\%}$ (mean ± SE)		*U*-test
	Polar night	Midnight sun	
C. obtusifrons	298 ± 52^{a}	609 ± 31^{a}	***
G. tenuispinus	381 ± 49^{a}	662 ± 26^{a}	***
G. brevispinus	791 ± 22^{b}	695 ± 34^{a}	**
A. multiserrata	628 ± 60^{b}	709 ± 43^{a}	ns
A. rostrata	1065 ± 68^{c}	1032 ± 182^{b}	ns
one-way ANOVA	***	***	

Within the species, temporal changes (polar night vs. midnight sun) were tested by the Mann-Whitney *U*-test. For inter-species comparison, one-way ANOVA and Tukey-Kramer test were performed for the data within the same period (polar night or midnight sun). Results of Tukey-Kramer tests are shown by the differences in the superscript alphabets. **$p < 0.01$, ***$p < 0.001$, ns: not significant.

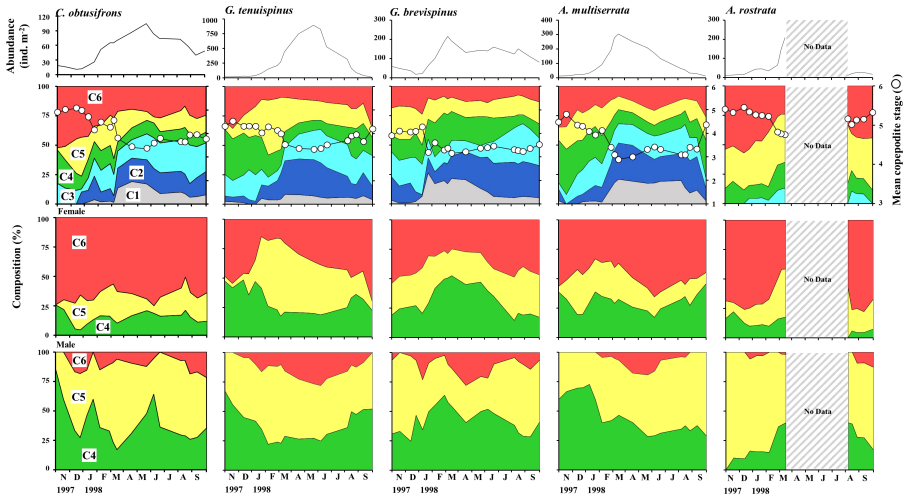

FIGURE 6
Seasonal changes in total abundance, stage composition, and population structure (for C4–C6) of females and males of the five dominant Aetideidae copepods in the western Arctic Ocean from 27 October 1997 to 29 September 1998. Mean copepodite stage (white circles) was calculated for each species for each sampling date. Populations of *Aetideopsis rostrata*, the deepest dwelling species, were not quantified between March and August 1998 because zooplankton collection was restricted to the shallower depths related to drifting of the ice station. The shallower dwelling species are *Chiridius obtusifrons*, *Gaetanus tenuispinus*, *G. brevispinus*, and *Aetideopsis multiserrata*.

δ^{15}N values were 13.4–15.4 somewhat lower than the polar night values within the species, although there was no significant difference between the polar night and the midnight sun. The species order in δ^{15}N values of the aetideid copepods was the same for the polar night and midnight sun.

4 Discussion

4.1. Vertical distribution

A schematic diagram of the seasonal vertical distributions and reproductive periods of the five aetideid copepods in the western Arctic Ocean is shown in Figure 7. During the midnight sun, the four species with the shallower distributions: *C. obtusifrons*, *G. tenuispinus*, *G. brevispinus*, and *A. multiserrata* were distributed at similar depths. However, during the polar night, *C. obtusifrons* and the two *Gaetanus* species changed their habitat depths (*C. obtusifrons* and *G. tenuispinus* ascended, whereas *G. brevispinus* descended), and their habitat depths were clearly separated during this period (Table 2). In contrast, the *A. rostrata* populations were distributed in deep waters throughout the year. Most of our knowledge about the vertical distribution of the aetideid copepods in the Arctic Ocean is derived from the summer season, particularly August–September; the end of the midnight sun. At this time, *C. obtusifrons* was reported to be distributed mainly at depths of 0–2,500 m, *G. tenuispinus* at 0–1,000 m, *G. brevispinus* at 100–2,000 m, and *A. rostrata* at 200–2,000 m (Kosobokova and Hirche, 2000; Laakmann et al., 2009a; Smoot and Hopcroft, 2017). Although little information is available for the vertical distribution of *A. multiserrata*, this species is treated as a meso- to bathypelagic species and was reported to distribute at depths of approximately 500–1,500 m (Richter, 1994; Richter, 1995). Thus, the vertical distribution ranges of the five aetideid copepods recorded in this study correspond with the reported vertical distribution depths in previous Arctic Ocean studies (Figure 5).

Information about the vertical distribution of aetideid copepods during the polar night is scarce. Moreover, limited information is available about the seasonal dynamics of their vertical distribution. As a notable exception, Richter (1994); Richter (1995) reported that there are no seasonal changes in the vertical distribution of Aetideidae in the Greenland Sea. In contrast to this Greenland Sea finding, results of the present study indicate that the four shallower-dwelling aedtideid copepods (*C. obtusifrons*, *G. tenuispinus*, *G. brevispinus*, and *A. multiserrata*) showed clear vertical depth separation during the polar night and exhibited seasonal vertical migration (Table 2). The coexistence mechanisms of the sympatric sibling copepods in the deep-sea of the Arctic Ocean are reported to include separation in vertical distribution and different food preferences (Laakmann et al., 2009a; Laakmann et al., 2009b; Laakmann and Auel, 2010). In terms of their feeding modes, the aetideid copepods are considered to be omnivores or detritivores and are reported to perform opportunistic feeding, utilising passive, sinking, particulate organic matter as their primary food sources (Richter, 1995; Auel, 1999; Sano et al., 2013; Sano et al., 2015). In the western Arctic Ocean, the amount of passive, sinking particle organic carbon flux is reported to be high for the midnight sun during spring to autumn, and low for the polar

TABLE 3 Sex ratio (% of females in total population) of the five Aetideidae copepods abundant in the western Arctic Ocean during October 1996 to September 1997.

Species Stage	Females in total (%) (mean ± SD)
Chiridius obtusifrons	
C4	48.4 ± 12.8
C5	43.6 ± 13.1
C6	92.9 ± 4.7
Total (C4–C6)	61.6 ± 10.2
Gaetanus tenuispinus	
C4	54.3 ± 11.9
C5	42.9 ± 11.3
C6	76.3 ± 15.6
Total (C4–C6)	57.8 ± 13.0
Gaetanus brevispinus	
C4	45.6 ± 9.0
C5	43.4 ± 9.8
C6	80.7 ± 13.5
Total (C4–C6)	56.6 ± 10.7
Aetideopsis multiserrata	
C4	57.6 ± 11.1
C5	46.7 ± 18.2
C6	95.8 ± 4.9
Total (C4–C6)	66.7 ± 11.4
Aetideopsis rostrata	
C4	47.7 ± 26.8
C5	35.7 ± 10.6
C6	97.3 ± 3.7
Total (C4–C6)	60.3 ± 13.7

Values are mean ± SD.

night during winter (O'Brien et al., 2006; Honjo et al., 2010). These seasonal changes in the amount of sinking particle flux may explain the seasonal vertical distribution of the sympatric aetideid copepods. It may be that during the midnight sun, a sufficiently high availability of sinking particles may provide sufficient food resources to support all four of the aetideid copepods, thus enabling their distribution and coexistence at similar depths. However, during the polar night, because of the low amount of sinking particles available across the depth range, the four copepod species may separate their habitat depths to reduce competition for food resources, a dynamic that may function as niche separation. Vertical separation in habitat depths and preference for carnivory are reported for the aetideid copepods (Laakmann et al., 2009a; Laakmann et al., 2009b; Laakmann and Auel, 2010).

4.2. Population structure

In this study, seasonal changes in population structure were observed for four of the aetideid copepods, except *A. rostrata*. The low MCS values indicated that population recruitment occurred for each species, and, common to all species, the seasonal timing of the low MCS values corresponded closely with the seasonal timing of the abundance peak of each species (Figure 6). By combining the timing of recruitment of early copepodite stages and the time taken for development of the eggs and nauplii, the seasonal reproduction period of each species can be estimated (Yamaguchi et al., 2020). Regarding aetideid copepod reproduction, egg diameters have been reported as 315 ± 10 μm (mean ± 1sd) for *G. tenuispinus*, 440 ± 66 μm for *G. brevispinus*, 290 ± 12 μm for *C. obtusifrons*, and 270–300 μm (range) for *A. rostrata* (Kosobokova et al., 2007), and it has been observed that the development time of early copepod stages is affected by temperature, food availability, and body size (egg diameter) (Mauchline, 1998). Because the egg diameters of the deep-sea aetideid copepods are much larger compared to those of the surface-dwelling copepods, their naupliar stages are suggested to be able to develop without feeding (Kosobokova et al., 2007). These facts indicate that the development times of eggs and nauplii could be estimated by two factors: habitat temperature and body size (egg diameter).

The relationships between temperature and the development time of early mesopelagic copepod stages with non-feeding naupliar stages have been reported for *Gaetanus variabilis* (= *Gaidius variabilis*) and *Paraeuchaeta elongata*, which have egg diameters of 325 ± 11 μm (*G. variabilis*) and 460 ± 30 μm (*P. elongata*) (Ozaki and Ikeda, 1997; Yamaguchi and Ikeda, 2000). These egg sizes are comparable to those of the aetideid copepods researched in this study (270–440 μm). Applying published Bělehrádek equations for *G. variabilis* and *P. elongata* (Ozaki and Ikeda, 1997; Yamaguchi and Ikeda, 2000) and habitat temperature of the aetideid copepods in this study: 0.57°C (mean temperature below 300 m; range: −0.23 to 1.07°C, Figure 3), the development times for eggs and nauplii to reach C1 are estimated to be 67.6–83.1 days. From field data, the recruitment of early copepodite stages was observed to be April–May for *C. obtusifrons* and *G. tenuispinus*, January–March for *G. brevispinus*, and February–March for *A. multiserrata* (Figure 6). Considering the estimated development time of eggs and nauplii (67.6–83.1 days), the reproductive period of each species was back-calculated as: February–March for *C. obtusifrons* and *G. tenuispinus*, November–January for *G. brevispinus*, and December–January for *A. multiserrata* (Figure 7). These reproductive periods corresponded with the timing of the polar night or occurred during the sunlight recovery season in the field.

Of the factors that determine the timing of copepod reproduction, food availability is known to be the most important (cf. Mauchline, 1998). At the SHEBA ice station, increases in phytoplankton and microplankton were reported to occur from late May to June (Sherr and Sherr, 2003; Sherr et al., 2003). This period corresponds with the growth season of the early copepodite stages of the aetideid species observed in this

study (Figure 6). Thus, as an energy source for the initiation of the reproduction of the aetideid copepods, other food resources may be important. Although Aetideidae species are known to be omnivorous, the importance of carnivorous feeding has been reported, especially for the adult stages, and their food is reported to comprise the energy-rich eggs and nauplii of the large-sized *Calanus* copepods, and adults of small-sized copepods such as *Microcalanus* and *Pseudocalanus* species (Richter, 1995; Auel, 1999; Sano et al., 2013; Sano et al., 2015). These carnivorous feeding modes of the aetideid copepods have been confirmed by fatty acid analysis (Laakmann et al., 2009a; Laakmann et al., 2009b; Laakmann and Auel, 2010). These facts suggest that the link between food resource availability and the initiation of reproduction of four of the aetideid copepods investigated in this study may be related to carnivorous feeding on small-sized copepods. Since $\delta^{15}N$ values of adult females were higher for *C. obtusifrons* and *Aetideopsis* spp. than those of *Gaetanus* spp., the carnivorous feeding modes would be more pronounced for the former species. And common for all aetideid copepods, carnivorous feeding modes were more common during the polar night than those in the midnight sun (Table 4).

In the present study, the reproduction of the four shallower-dwelling aetideid copepods could be classified into two types based on vertical distribution and seasonality (Figure 7). In the first type of reproduction, exhibited by *C. obtusifrons* and *G. tenuispinus*, both species ascended to shallower depths during the polar night, and their reproductive period occurred from the end of the polar night into the sunlight recovery period (Figure 7). The timing of reproduction of these species corresponded with the seasonal population increase of the small-sized and abundant copepod: *Microcalanus pygmaeus* (Ashjian et al., 2003). Since *M. pygmaeus* is distributed mainly in the upper mesopelagic layer (Auel and Hagen, 2002; Ashjian et al., 2003), the upward migration of *C. obtusifrons* and *G. tenuispinus* during the polar night may be an adaptive strategy for prey capture at shallower depths, which may provide an important energy source to support their reproduction. The other type of reproduction was exhibited by *G. brevispinus* and *A. multiserrata*. Both these species remained in deeper waters, even during the polar night, and began reproducing at the beginning of the polar night (Figure 7), which was comparatively earlier than for the two shallower-dwelling species. The timing of reproduction of these two deeper-dwelling species corresponded with the timing in reproduction of the large-sized copepod *Calanus hyperboreus*, which dominates the zooplankton biomass in part of the Arctic Ocean (Conover and Huntley, 1991; Hirche and Niehoff, 1996; Ashjian et al., 2003). During the winter to spring period, *C. hyperboreus* descends to the mesopelagic layer and sheds floating eggs (Conover and Huntley, 1991; Hirche and Niehoff, 1996; Ashjian et al., 2003). To perform raptorial feeding on the eggs and nauplii of *C. hyperboreus*, the two deeper-dwelling aetideid copepods, *G. brevispinus* and *A. multiserrata*, may remain at the deeper depths during the polar night in order to use the abundance of *C. hyperboreus* eggs and nauplii as their main energy source for reproduction. These seasonal trends in feeding modes were evidenced by the $\delta^{15}N$ values of the aetideid adult specimens (Table 4). The differences in vertical distribution and timing of reproduction among the five sympatric aetideid copepods observed in this study may function to reduce interspecific competition within the resource-limited mesopelagic layers and could be a key mechanism maintaining high biodiversity at these depths in the Arctic Ocean.

5 Conclusions

In this study, we developed a set of metrics to aid species identification of early copepodite stages of five sympatric aetideid copepods (*Chiridius obtusifrons*, *Gaetanus tenuispinus*, *G. brevispinus*, *Aetideopsis multiserrata*, and *A. rostrata*), and evaluated vertical distribution and seasonal population structure of these species using a year-round sample time-series collected at the drifting ice station (SHEBA) in the western Arctic Ocean. Combinations of morphological characteristics (prosome length, cephalosome, and prosome widths) were used to identify the early

TABLE 4 Summary of $\delta^{15}N$ value (‰, mean ± SE) of five Aetideidae copepods in the western Arctic Ocean during the polar night and midnight sun.

	$\delta^{15}N$ (‰, mean ± SE)		
	Polar night	**Midnight sun**	***U*-test**
C. obtusifrons	15.4 ± 0.1^{c}	14.4 ± 0.1^{c}	ns
G. tenuispinus	14.1 ± 0.1^{a}	13.4 ± 0.1^{a}	ns
G. brevispinus	14.6 ± 0.1^{b}	13.8 ± 0.1^{b}	ns
A. multiserrata	16.4 ± 0.1^{d}	15.4 ± 0.1^{d}	ns
A. rostrata	15.4 ± 0.0^{c}	14.8^{c}	–
one-way ANOVA	***	***	

Within the species, temporal changes (polar night vs. midnight sun) were tested by the Mann-Whitney *U*-test. For inter-species comparison, one-way ANOVA and Tukey-Kramer test were performed for the data within the same period (polar night or midnight sun). Results of Tukey-Kramer tests are shown by the differences in the superscript alphabets. ***: $p<0.001$, ns: not significant.

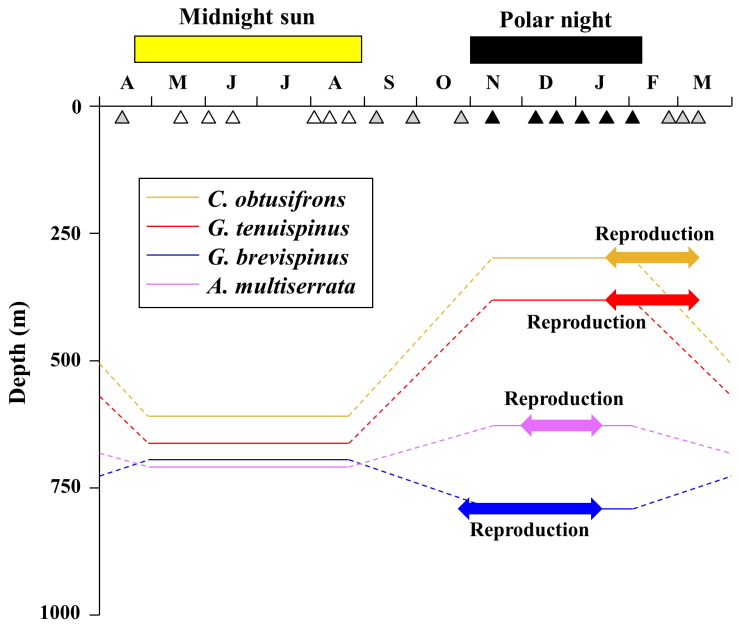

FIGURE 7
Schematic diagram showing seasonal changes in vertical distribution and timing of reproduction of four of the dominant Aetideidae copepods in the western Arctic Ocean. The open, solid, and grey triangles indicate the sampling dates during the midnight sun, polar night, and their transition periods, respectively. The shallower-dwelling species are *Chiridius obtusifrons*, *Gaetanus tenuispinus*, *G. brevispinus*, and *Aetideopsis multiserrata*.

copepodite stages to species. *Aetideopsis rostrata* was distributed in deep waters throughout the year. The other species distributed at similar depths during the midnight sun, whereas their vertical distribution varied with species during the polar night. Reproduction timing also varied among these four aetideid copepods and occurred at the start or at the end of the polar night, possibly related to food availability. Seasonal distribution dynamics and different reproductive periods may reduce interspecific competition among aetideid copepods in the Arctic Ocean.

Data availability statement

The original contributions presented in the study are included in the article/Supplementary Material. Further inquiries can be directed to the corresponding author.

Author contributions

YK, KT, CA, RC, and AY designed the study; CA and RC collected the samples; YK and KT analysed the samples; YK and AY analysed the data; YK and AY wrote the paper with contributions from all authors. All authors read and approved the final manuscript.

Funding

Collection of the samples was supported in part by grants #OCE9707184 to CA and #OCE9707182 to RC from the US National Science Foundation. This work was partially supported by the Arctic Challenge for Sustainability II (ArCS II), Program Grant Number JPMXD1420318865. This research was also supported by the Environment Research and Technology Development Fund (JPMEERF20214002) of the Environmental Restoration and Conservation Agency of Japan. In addition, this work was partly supported by a Grant-in-Aid for Challenging Research (Pioneering) JP20K20573, and Scientific Research JP20H03054 (B), JP19H03037 (B), JP21H02263 (B), and JP17H01483 (A) from the Japanese Society for the Promotion of Science (JSPS).

Acknowledgments

We thank the crew members of the CCGS *Des Groseilliers* and the SHEBA project members, most especially Harold "Buster" Welch, for assistance in collecting the samples and CTD data.

Conflict of interest

The authors declare that the research was conducted in the absence of any commercial or financial relationships that could be construed as a potential conflict of interest.

Publisher's note

All claims expressed in this article are solely those of the authors and do not necessarily represent those of their affiliated organizations, or those of the publisher, the editors and the reviewers. Any product that may be evaluated in this article, or claim that may be made by its manufacturer, is not guaranteed or endorsed by the publisher.

Supplementary material

The Supplementary Material for this article can be found online at: https://www.frontiersin.org/articles/10.3389/fmars.2022.943100/full#supplementary-material

References

Ashjian, C., and Campbell, R. (2007) *Mesozooplankton abundance and biomass. version 1.0* (UCAR/NCAR - Earth Observing Laboratory) (Accessed 27 Jun 2022).

Ashjian, C. J., Campbell, R. G., Welch, H. E., Butler, M., and VanKeuren, D. (2003). Annual cycle in abundance, distribution, and size in relation to hydrography of important copepod species in the western Arctic ocean. *Deep-Sea. Res. Part I.: Oceanogr. Res. Pap.* 50 (10–11), 1235–1261. doi: 10.1016/S0967-0637(03)00129-8

Auel, H. (1999). The ecology of Arctic deep-sea copepods (Euchaetidae and aetideidae). aspects of their distribution, trophodynamics and effect on the carbon flux. *Berichte. Zur. Polarforschung. (Report. Pol. Res.)* 319, 1–97. doi: 10.2312/BzP_0319_1999

Auel, H., and Hagen, W. (2002). Mesozooplankton community structure, abundance and biomass in the central Arctic ocean. *Mar. Biol.* 140 (5), 1013–1021. doi: 10.1007/s00227-001-0775-4

Brock, T. D. (1981). Calculating solar radiation for ecological studies. *Ecol. Model.* 14 (1–2), 1–19. doi: 10.1016/0304-3800(81)90011-1

Brodskii, K. A. (1950). Calanoida of the far Eastern seas and polar basin of the USSR. *Key. To. Fauna. USSR.* 35, 1–440.

Conover, R. J., and Huntley, M. (1991). Copepods in ice-covered seas–distribution, adaptations to seasonally limited food, metabolism, growth patterns and life cycle strategies in polar seas. *J. Mar. Syst.* 2 (1–2), 1–41. doi: 10.1016/0924-7963(91)90011-l

Dilling, L., Wilson, J., Steinberg, D., and Alldredge, A. (1998). Feeding by the euphausiid *Euphausia pacifica* and the copepod *Calanus pacificus* on marine snow. *Mar. Ecol. Prog. Ser.* 170, 189–201. doi: 10.3354/meps170189

Goetze, E. (2003). Cryptic speciation on the high seas; global phylogenetics of the copepod family eucalanidae. *Proc. R. Soc. Lond. Ser. B.: Biol. Sci.* 270 (1531), 2321–2331. doi: 10.1098/repb.2003.2505

Hirche, H. J., and Niehoff, B. (1996). Reproduction of the Arctic copepod *Calanus hyperboreus* in the Greenland Sea-field and laboratory observations. *Pol. Biol.* 16 (3), 209–219. doi: 10.1007/BF02329209

Honjo, S., Krishfield, R. A., Eglinton, T. I., Manganini, S. J., Kemp, J. N., Doherty, K., et al. (2010). Biological pump processes in the cryopelagic and hemipelagic Arctic ocean: Canada basin and chukchi rise. *Prog. Oceanogr.* 85 (3–4), 137–170. doi: 10.1016/j.pocean.2010.02.009

Horton, T., Marsh, L., Bett, B. J., Gates, A. R., Jones, D. O. B., Benoist, N. M. A., et al. (2021). Recommendations for the standardisation of open taxonomic nomenclature for image-based identifications. *Front. Mar. Sci.* 8. doi: 10.3389/fmars.2021.620702

Kosobokova, K., and Hirche, H. J. (2000). Zooplankton distribution across the lomonosov ridge, Arctic ocean: species inventory, biomass and vertical structure. *Deep-Sea. Res. Part I : Oceanogr. Res. Pap.* 47 (11), 2029–2060. doi: 10.1016/S0967-0637(00)00015-7

Kosobokova, K. N., Hirche, H. J., and Hopcroft, R. R. (2007). Reproductive biology of deep-water calanoid copepods from the Arctic ocean. *Mar. Biol.* 151 (3), 919–934. doi: 10.1007/s00227-006-0528-5

Kosobokova, K. N., and Hopcroft, R. R. (2010). Diversity and vertical distribution of mesozooplankton in the arctic's Canada basin. *Deep-Sea Res* Part. *II: Trop. Stud. Oceanogr.* 57 (1–2), 96–110. doi: 10.1016/j.dsr2.2009.08.009

Kosobokova, K. N., Hopcroft, R. R., and Hirche, H. J. (2011). Patterns of zooplankton diversity through the depths of the arctic's central basins. *Mar. Biodivers.* 41 (1), 29–50. doi: 10.1007/s12526-010-0057-9

Laakmann, S., and Auel, H. (2010). Longitudinal and vertical trends in stable isotope signatures ($\delta^{13}C$ and $\delta^{15}N$) of omnivorous and carnivorous copepods across the south Atlantic ocean. *Mar. Biol.* 157, 463–471. doi: 10.1007/s00227-009-1332-9

Laakmann, S., Kochzius, M., and Auel, H. (2009a). Ecological niches of Arctic deep-sea copepods: Vertical partitioning, dietary preferences and different trophic levels minimize inter-specific competition. *Deep-Sea. Res. Part I : Oceanogr. Res. Pap.* 56 (5), 741–756. doi: 10.1016/j.dsr.2008.12.017

Laakmann, S., Stumpp, M., and Auel, M. (2009b). Vertical distribution and dietary preferences of deep-sea copepods (Euchaetidae and aetideidae; calanoida) in the vicinity of the Antarctic polar front. *Pol. Biol.* 32 (5), 679–689. doi: 10.1007/s00300-008-0573-2

Lee, C. E. (2000). Global phylogeography of a cryptic copepod species complex and reproductive isolation between genetically proximate "populations". *Evolution* 54 (6), 2014–2027. doi: 10.1111/j.0014-3820.2000.tb01245.x

Lowry, L. F., Sheffield, G., and George, C. (2004). Bowhead whale feeding in the alaskan Beaufort Sea, based on stomach contents analyses. *J. Cetacean. Res. Manage.* 6 (3), 215–223.

Marin, V. (1987). The oceanographic structure of the eastern Scotia–IV. distribution of copepod species in relation to hydrography in 1981. *Deep-Sea. Res. Part A. Oceanogr. Res. Pap.* 34 (1), 105–121. doi: 10.1016/0198-0149(87)90125-7

Markhaseva, E. L. (1996). Calanoid copepods of the family aetideidae of the world ocean. *Proc. Zool. Inst. Russian Acad. Sci. St. Petersburg.* 268, 1–331.

Mauchline, J. (1998). The biology of calanoid copepods. *Adv. Mar. Biol.* 33, 1–710.

Norris, R. D. (2000). Pelagic species diversity, biogeography, and evolution. *Paleobiology* 26 (S4), 236–258. doi: 10.1017/S0094837300026956

O'Brien, M. C., Macdonald, R. W., Melling, H., and Iseki, K. (2006). Particle fluxes and geochemistry on the Canadian Beaufort shelf: Implications for sediment transport and deposition. *Continent. Shelf. Res.* 26 (1), 41–81. doi: 10.1016/j.csr.2005.09.007

Ozaki, K., and Ikeda, T. (1997). The effect of temperature on the development of eggs and nauplii of the mesopelagic copepod *Paraeuchaeta elongata*. *Plankt. Biol. Ecol.* 44 (1/2), 91–95.

Pennak, R. W. (1943). An effective method of diagramming diurnal movements of zooplankton organisms. *Ecology* 24 (3), 405–407. doi: 10.2307/1930542

Richter, C. (1994). Regional and seasonal variability in the vertical distribution of mesozooplankton in the Greenland Sea. *Berichte. Zur. Polarforschung. (Report. Pol. Res.)* 154, 1–87. doi: 10.2312/BzP_0154_1994

Richter, C. (1995). Seasonal changes in the vertical distribution of mesozooplankton in the Greenland Sea gyre (75°N): distribution strategies of calanoid copepods. *ICES J. Mar. Sci.* 52 (3–4), 533–539. doi: 10.1016/1054-3139(95)80067-0

Sano, M., Maki, K., Nishibe, Y., Nagata, T., and Nishida, S. (2013). Feeding habits of mesopelagic copepods in sagami bay: Insights from integrative analysis. *Prog. Oceanogr.* 110, 11–26. doi: 10.1016/j.pocean.2013.01.004

Sano, M., Nishibe, Y., Tanaka, Y., and Nishida, S. (2015). Temporally sustained dietary niche partitioning in two mesopelagic copepod species and their mouthpart morphology. *Mar. Ecol. Prog. Ser.* 518, 51–67. doi: 10.3354/meps11045

Sherr, B. F., and Sherr, E. B. (2003). Community respiration/production and bacterial activity in the upper water column of the central Arctic ocean. *Deep-Sea. Res. Part I : Oceanogr. Res. Pap.* 50 (4), 529–542. doi: 10.1016/S0967-0637(03) 00030-X

Sherr, E. B., Sherr, B. F., Wheeler, P. A., and Thompson, K. (2003). Temporal and spatial variation in stocks of autotrophic and heterotrophic microbes in the upper water column of the central Arctic ocean. *Deep-Sea. Res. Part I : Oceanogr. Res. Pap.* 50 (5), 557–571. doi: 10.1016/S0967-0637(03)00031-1

Smoot, C. A., and Hopcroft, R. R. (2017). Depth-stratified community structure of Beaufort Sea slope zooplankton and its relations to water masses. *J. Plankt. Res.* 39 (1), 79–91. doi: 10.1093/plankt/fbw087

Thibault, D., Head, E. J. H., and Wheeler, P. A. (1999). Mesozooplankton in the Arctic ocean in summer. *Deep-Sea. Res. Part I : Oceanogr. Res. Pap.* 46 (8), 1391–1415. doi: 10.1016/S0967-0637(99)00009-6

Wassmann, P., Reigstad, M., Haug, T., Rudels, B., Carroll, M. L., Hop, H., et al. (2006). Food webs and carbon flux in the barents Sea. *Prog. Oceanogr.* 71 (2–4), 232–287. doi: 10.1016/j.pocean.2006.10.003

Wilson, S. E., Steinberg, D. K., Chu, F. L. E., and Bishop, J. K. B. (2010). Feeding ecology of mesopelagic zooplankton of the subtropical and subarctic north pacific ocean determined with fatty acid biomarkers. *Deep-Sea. Res. Part I : Oceanogr. Res. Pap.* 57 (10), 1278–1294. doi: 10.1016/j.dsr.2010.07.005

Yamaguchi, A., Ashjian, C. J., Campbell, R. G., and Abe, Y. (2020). Vertical distribution, population structure and developmental characteristics of the less studied but globally distributed mesopelagic copepod *Scaphocalanus magnus* in the western Arctic ocean. *J. Plankt. Res.* 42 (3), 368–377. doi: 10.1093/plankt/fbaa021

Yamaguchi, A., and Ikeda, T. (2000). Vertical distribution, life cycle, and developmental characteristics of the mesopelagic calanoid copepod *Gaidius variabilis* (Aetideidae) in the oyashio region, western north pacific ocean. *Mar. Biol.* 137 (1), 99–109. doi: 10.1007/s002270000316

Zhang, J., Spitz, Y. H., Steele, M., Ashjian, C., Campbell, R., Berline, L., et al. (2010). Modeling the impact of declining sea ice on the Arctic marine planktonic ecosystem. *J. Geophys. Res.: Ocean.* 115, C10015. doi: 10.1029/2009JC005387